Synthesis of Non-Al-Containing Hydrotalcite-like Compound $Mg_{0.3}Co^{II}_{0.6}Co^{III}_{0.2}(OH)_2(NO_3)_{0.2}\cdot H_2O$

H. C. Zeng,* Z. P. Xu, and M. Qian

Department of Chemical Engineering, Faculty of Engineering National University of Singapore, 10 Kent Ridge Crescent, Singapore 119260

Received April 3, 1998. Revised Manuscript Received June 1, 1998

Hydrotalcite-like compound (HTlc) of $Mg_{0.3}Co^{II}_{0.6}Co^{III}_{0.2}(OH)_2(NO_3)_{0.2}\cdot H_2O$ has been synthesized for the first-time by coprecipitation in an ammoniacal solution and hydrothermal treatments under various O_2:N_2 atmospheres. Using elemental analysis and redox titration, it is found that about 23% of the original Co^{2+} is oxidized to Co^{3+}, resulting in formation of HTl structure. Related to the Co^{3+} content, intercalation of NO_3^- anion is observed. The X-ray diffraction pattern shows a conversion from brucite-like to HTl structures with increase of O_2 partial pressure. Using different drying schemes (25 and 60 °C) and differential scanning calorimetry analysis, it is found that the thermal stability of the HTlcs is proportional to the Mg content. Higher specific surface areas are observed for decomposed products with low Co/Mg ratio. A trace amount of Co_3O_4 is also detected by FTIR for samples synthesized under high O_2 partial pressures, which can be attributed to a deeper oxidation of Co^{2+}. Thermodynamic considerations are also given to the redox reactions in both aqueous and solid phases.

Introduction

Co,Al-containing hydrotalcite-like compounds (HTlcs) stand as an interesting family in layered double hydroxide materials.[1−9] The increasing research activity in this area is due not only to fundamental interest in HTlcs[2−5] but also to many potential applications of the materials such as syntheses of alcohols and hydrocarbons in heterogeneous catalysis[6,7] and decomposition of greenhouse gas N_2O in environmental catalysis.[8,9]

In these HTlcs, Co has been classified as a bivalent cation to replace Mg^{2+} in the natural hydrotalcite compound Mg,Al-HT, whereas Al^{3+} has been considered to be responsible for anion intercalation due to its extra +1 charge over the bivalent Co^{2+} in the brucite-like layer. No study has been devoted to investigate whether Co^{2+} is strictly divalent in the brucite-type layers or may also contribute partially to the anion intercalation like its trivalent counterpart Al^{3+}. It is noted that in these materials Al is an essential element to construct HTlcs. However, if some Co in the brucite-type layers adopts the oxidation state of +3, it is then possible to build HTlcs by using another type of cation combination, Mg + Co, where no Al is needed. In this type of proposed molecular architecture, low corrugation within a Mg,Co-brucite-like sheet would be expected, since the cation radii of Mg^{2+} and Co^{3+} are quite similar (0.65 and 0.63 Å respectively).[1]

Regarding their catalytic applications, activity created by the Mg,Co-HTlcs (if possible) should be different from that of the Co,Al-HTlcs since composition determines ultimate performance of a catalyst. For example, consider a simple segment of metal−oxygen−metal (M−O−M′) in calcined HTlcs (oxides). Owing to different effective charges and polarizibilities of the cations, Mg^{2+}−O−$Co^{2+,3+}$ and $Co^{2+,3+}$−O−Al^{3+} will be expected to perform differently concerning a charge-transfer mechanism between these units and an adsorbed species. For example, regarding adsorption applications of Mg,Co-HTlcs in replacement of the Co,Al-HTlcs, one would expect a change in the acid−base properties of the calcined oxides, as the group IIIA metal Al is amphoteric while the alkali earth metal Mg is basic.

Recently, we have synthesized Mg,Co metal oxides for the catalytic decomposition of N_2O, which shows high activity for low-temperature operation.[10] To study fundamentals of HTlc and further design of Mg,Co-oxides for the N_2O decomposition and other catalytic applications, the current work aims at developing a synthetic method to obtain single-phase non-Al-containing Mg,Co-HTlcs using controlled O_2:N_2 atmospheres. Furthermore, this work also looks into the thermal evolution of non-Al-containing HTlcs in the preparation of catalytic metal oxide materials.[11]

* Corresponding author.

(1) Cavani, F.; Trifiro, F.; Vaccari, A. *Catal. Today* **1991**, *11*, No. 2, 173.
(2) Reichle, W. T. *Solid State Ionics* **1986**, *22*, 135.
(3) Ulibarri, M. A.; Fernandez, J. M.; Labajos, F. M.; Rives, V. *Chem. Mater*. **1991**, *3*, 626.
(4) Kannan, S.; Swamy, C. S. *J. Mater. Sci. Lett*. **1992**, *11*, 1585.
(5) Tsuji, M.; Mao, G.; Yoshida, T.; Tamaura, Y. *J. Mater. Res*. **1993**, *8*, 1137.
(6) Porta, P.; Morpurgo, S.; Pettiti, I. *J. Solid State Chem*. **1996**, *121*, 372.
(7) Morpurgo, S.; Jacono, M. L.; Porta, P. *J. Solid State Chem*. **1996**, *122*, 324.
(8) Kannan, S.; Swamy, C. S. *Appl. Catal. B* **1994**, *3*, 109.
(9) Armor, J. N.; Braymer, T. A.; Li, Y.; Petrocelli, E. P.; Weist, E. L.; Kannan, S.; Swamy, C. S. *Appl. Catal. B* **1996**, *7*, 397.
(10) Qian, M.; Zeng, H. C. *J. Mater. Chem*. **1997**, *7*, 493.
(11) Labajos, F. M.; Rives, V. *Inorg. Chem*. **1996**, *35*, 5313.

S0897-4756(98)00250-6 CCC: $15.00
Published on Web 07/22/1998

Table 1. Atmosphere-Controlled Preparation Conditions for Synthesis of Samples 1−10

no.	precip atmos (O_2:N_2)[a]	aging temp/time (°C/h)[b]	drying temp/time (°C/h)	structural phase (by XRD)[c]
1	0:4	65/18	25/18	brucite-like
2	0:4	65/18	60/18	brucite-like
3	1:3	65/18	25/18	brucite-like + hydrotalcite-like
4	1:3	65/18	60/18	brucite-like + hydrotalcite-like
5	2:2	65/18	25/18	hydrotalcite-like
6	2:2	65/18	60/18	hydrotalcite-like
7	3:1	65/18	25/18	hydrotalcite-like
8	3:1	65/18	60/18	hydrotalcite-like
9	4:0	65/18	25/18	hydrotalcite-like
10	4:0	65/18	60/18	hydrotalcite-like

[a] Total gas ($O_2 + N_2$) flow-rate = 40 mL/min. [b] O_2:N_2 means flow rate ratio of oxygen to nitrogen in each $O_2 + N_2$ combination, e.g., 0:4 = (0 mL of O_2/min):(40 mL of N_2 /min). [c] Structural phases (by XRD) for the materials are also included for easy reference.

Experimental Section

Materials Preparation. Mg−Co−NO_3 hydrotalcite-like compounds were prepared using a coprecipitation method in ammoniacal solution. Sample preparation conditions in this work are summarized in Table 1 for easy reference. Briefly, 250.0 mL of ammonia solution (0.5 M) was filled into a three-necked round-bottom flask, which was then bubbled with $O_2 + N_2$ gas in various combinations (Table 1) at a total flow rate of 40 mL/min. A 50-mL mixed nitrate aqueous solution of Mg−Co (total cation concentration = 1.0 M; $Mg(NO_3)_2 \cdot 6H_2O$, >99.0%, Merck; $Co(NO_3)_2 \cdot 6H_2O$, >99.0%, Fluka) with a molar ratio of 1:1 was added rapidly to each of the above atmosphere-controlled ammoniacal solutions within 1 min. The whole system (precipitate + solution) was gradually heated to 65 °C and refluxed (i.e., thermal treatment) at the same temperature for 18 h under each $O_2 + N_2$ combination. The system was then brought back to room temperature while the gas flow was still on. Throughout the course of each experiment, good mixing was maintained using a magnetic stirrer. Initial and final pH values for the solution phase were determined to be 9.5 and 8.5, respectively. After the above hydrothermal treatment, Mg−Co−NO_3 precipitates were obtained by filtrating and thorough washing with deionized water. Each as-prepared precipitate was divided into two equal parts respectively for further thermal treatment (drying).

Two drying schemes were adopted: (i) drying inside a fumehood at 25 °C for 18 h (samples 1, 3, 5, 7, and 9, Table 1) and (ii) drying at 60 °C in an electric oven with stagnant air for 18 h (samples 2, 4, 6, 8, and 10, Table 1).

The Co^{3+} content was determined by a redox titration method. A solid sample (10.00 mg) was dissolved in 20.0 mL of 1.0 M HCl solution with the assistance of gentle heating. The produced Cl_2 gas was gradually purged by N_2 (60 mL/min) into 50.0 mL of 0.01 M KI solution mixed with starch indicator. The resultant blue mixture was then titrated against a $Na_2S_2O_3$ solution (0.0100 M) till disappearance of the blue coloration.

Materials Characterization. The chemical composition of the prepared samples was investigated by elemental analysis (EA) with a Labtam Plasmascan F10 instrument (ICP) and a Perkin-Elmer 2400 CHN analyzer. The crystallographic information on the samples was obtained by using an X-ray diffraction (XRD) method. Diffraction intensity versus 2θ data were measured in a Shimadzu XRD-6000 X-ray diffractometer operating at 40 kV/30 mA with Cu Kα radiation (λ = 1.5418 Å) from 5° to 55° at a scanning rate of 1°/min.[12] Chemical bonding of metal−oxygen, hydroxy, and intercalated functional groups (anions) was studied with Fourier transform infrared spectroscopy (FTIR, Shimadzu FTIR-8101) using the potassium bromide (KBr) pellet technique. The spectrum background was corrected with a freshly prepared pure KBr pellet. Forty scans were performed for each spectrum to ensure a good signal/noise ratio.[12]

A differential scanning calorimetry (DSC, Netzsch DSC200) study was further conducted to investigate the thermal decomposition of the precipitate samples. DSC measurements were carried out from 40 to 500 °C at a scanning rate of 10 °C/min under a nitrogen atmosphere with a gas flow rate of 15 mL/min. Surface areas of calcined samples at 200 and 400 °C were determined by N_2 adsorption−desorption in a NOVA1000 instrument, using the BET method.[10]

Results and Discussion

Synthesis and Chemical Composition. In the current work, two variable synthesis parameters were used: (i) oxygen and nitrogen molar ratio in the gas flow and (ii) drying temperature. The former parameter creates different chemical environments for the synthesis in aqueous phase, and the latter provides different thermal conditions for the prepared wet HTlc to dehydrate or to interact with ambient chemical species such as CO_2. It should be mentioned that different O_2:N_2 molar ratios correspond to different oxygen partial pressure in synthesis, since all experiments were conducted at normal pressure. On the basis of EA and XRD/FTIR investigations (which will be presented later), the general chemical formula for the HTlcs in this work can be written quantitatively as $Mg_aCo^{II}_bCo^{III}_c(OH)_d(NO_3)_e(CO_3)_f \cdot nH_2O$, whose coefficients ($a$ through n) are listed in Table 2 for some representative samples studied. As can be seen, chemical compositions of the precipitates change substantially, in response to the preparative atmosphere. For example, Co^{3+} cations are found in all O_2-involving syntheses (samples 3−10; see Table 1 for experimental conditions), while it is not detectable in samples 1 and 2, which were prepared under an inert atmosphere (Table 2). In particular, anion NO_3^- anions are more abundant in samples synthesized under higher O_2 partial pressures. Based on EA results, the Co/Mg molar ratios in samples 1−4, 9, and 10 are lower than those in samples 5−8. For the reported two pairs of samples (1 vs 2, and 9 vs 10), the drying temperature causes no difference in Co/Mg ratio [$(b + c)/a$, Table 2] and anion contents (NO_3^- and CO_3^{2-}), since these chemical species are determined solely during the aqueous phase synthesis. In all cases, however, water contents in 60 °C-dried samples are systematically lower than those dried at 25 °C (Table 2), because the higher temperature accelerates the drying process. It is noted that the carbon contents (at low level) in all samples are quite similar, regardless of the atmosphere and the drying scheme employed. Hence, it is considered that they are mainly contaminants due to dissolution of ambient carbon dioxide during the sample preparation and drying.

As the above preparative parameters cause a great difference in chemical composition, the structural and thermal properties of the final products will be further studied in the following sections. In view of the gradual increase of Co^{3+} and anion species NO_3^- in the precipitates with higher partial pressure of oxygen, redox reactions occurring in both aqueous phase and gas phase will be considered next.

Thermodynamic Consideration. The ammoniacal solution used in this work determines a number of

(12) Zeng, H. C.; Tung, S. K. *Chem. Mater.* **1996**, *8*, 2667.

Table 2. Elemental Analysis Results for the Samples 1, 2, 9, and 10[a]

no.	Mg^{2+} (*a*)	Co^{2+} (*b*)	Co^{3+} (*c*)	OH^- (*d*)	NO_3^- (*e*)	CO_3^{2-} (*f*)	H_2O (*n*)	structural phase
1[b]	0.342	0.791	0	2.225	0.003	0.018	0.331	brucite-like
2	0.350	0.809	0	2.280	0.005	0.017	0.208	brucite-like
9[c]	0.244	0.487	0.142	1.682	0.169	0.018	0.932	hydrotalcite-like
10	0.257	0.500	0.148	1.749	0.163	0.023	0.796	hydrotalcite-like

[a] The letters *a* through *n* are coefficients (before normalization) in the general formula $Mg_aCo^{II}_bCo^{III}_c(OH)_d(NO_3)_e(CO_3)_f\cdot nH_2O$. [b] On the basis of data of samples 1 and 2, the normalized formula for the brucite-like compound is $[Mg_{0.3}Co^{II}_{0.7}(OH)_2]\cdot 0.2H_2O$ (estimated error for *a* through *n*: $<\pm 0.1$). [c] On the basis of data of samples 9 and 10, the normalized formula for the HTlc is $Mg_{0.3}Co^{II}_{0.6}Co^{III}_{0.2}(OH)_2(NO_3)_{0.2}\cdot H_2O$ (estimated error for *a* through *n*: $<\pm 0.1$).

chemical reactions in the aqueous phase. First, it provides a basic medium (OH^-) for hydroxide synthesis. Second, it gives away complexing agent NH_3 to water-coordinated cation $[Co(H_2O)_6]^{2+}$ (or Co^{2+} for simplicity) to form a new complex $[Co(NH_3)_6]^{2+}$, because the ligand strength of NH_3 is stronger than that of H_2O.[13] Under current preparation conditions, Co^{2+} can be oxidized to Co^{3+} in both aqueous and solid phases. On one hand, the resultant $[Co(NH_3)_6]^{2+}$ in the liquid phase can be easily oxidized to $[Co(NH_3)_6]^{3+}$ because of the low standard reduction potential ($E°$):[14]

$$[Co(NH_3)_6]^{3+} + e = [Co(NH_3)_6]^{2+} \qquad E° = 0.11\ V \quad (1)$$

On the other hand, $Co(OH)_2$ can be oxidized to $Co(OH)_3$ [or CoO(OH)] within the forming precipitate (solid phase) in basic media:[14,15]

$$Co(OH)_3(s) + e = Co(OH)_2(s) + OH^- \qquad E° = 0.17\ V \quad (2.1)$$

or

$$CoO(OH)(s) + H_2O + e = Co(OH)_2(s) + OH^- \qquad E° = 0.17\ V \quad (2.2)$$

Although the oxidation of $[Co(H_2O)_6]^{2+}$ to $[Co(H_2O)_6]^{3+}$ is highly unfavorable in aqueous solution,[14] the above half-reactions open new routes to obtain Co^{3+} if a suitable oxidant is available. In this regard, laboratory oxygen (which has been used in the current work) can meet this requirement considering its intermediate oxidizing power in basic media:[15]

$$^1/_4O_2 + {}^1/_2H_2O + e = OH^- \qquad E° = 0.40\ V \quad (3)$$

In view of low concentrations for all solutes, especially for O_2 gas, the current synthesis system can be treated as an ideally dilute solution. Applying Henry's law to the current work, Figure 1 gives the calculated molar fraction (X) of O_2 in an aqueous solution of 65 °C as a function of O_2 partial pressure. Apparently, dissolving O_2 has a linear relationship with its external partial pressure. Concerning the oxidation of Co^{2+} in solid $Co(OH)_2$ with O_2 in the current case, the following reaction can be written from eqs 2.1 and 3:

$$^1/_4O_2 + {}^1/_2H_2O + Co(OH)_2(s) = Co(OH)_3(s) \quad (4)$$

The free energy change (ΔG) of above reaction at 65 °C is calculated by using the Nernst equation, and the

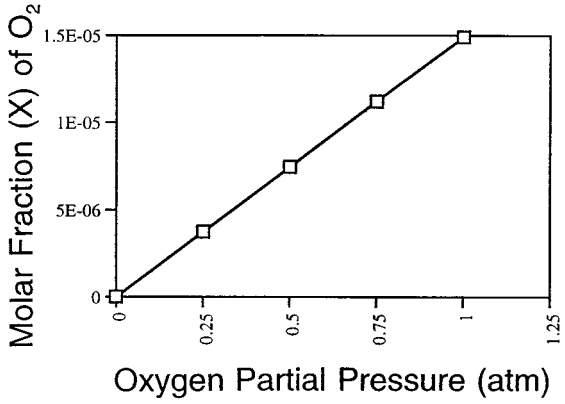

Figure 1. Molar fraction (X) of O_2 in aqueous solution at 65 °C under O_2 partial pressures of 0.0−1.0 atm.

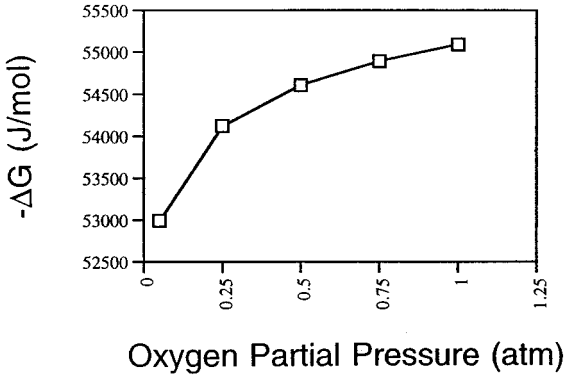

Figure 2. Free energy calculations from eq 4 under O_2 partial pressures of 0.05−1.00 atm.

calculation results are plotted in Figure 2. Unlike the linear molar fraction line (X, Figure 1), $-\Delta G$ increases more abruptly at low P_{O_2} while leveling off at higher P_{O_2}. Thermodynamically, one will be able to sense the driving force of the above redox reaction under the different P_{O_2} from this curve.

The formation of $[Co(NH_3)_6]^{3+}$ in aqueous phase should be further considered. Since this complex is very stable under basic conditions (dissociation constants $K_d = 9 \times 10^{-6}$ for $[Co(NH_3)_6]^{2+}$ and $K_d = 5 \times 10^{-35}$ for $[Co(NH_3)_6]^{3+}$),[16] one may expect that a significant amount of Co in the form of $[Co(NH_3)_6]^{3+}$ or other complexes[14] is still in the aqueous phase for low Co/Mg ratio [$(b + c)/a$, Table 2] precipitate cases (samples 9 and 10). Without considering this fact as well as other solution equilibria, simple explanation based only on solubility

(13) Mahan, B. M.; Myers, R. J. *University Chemistry*; Benjamin/Cummings, Menlo Park, CA, 1987; p 815.
(14) Cotton, F. A.; Wilkinson, G. *Advanced Inorganic Chemistry*; John Willey & Sons: New York, 1980; Chapter 21, p 768.
(15) Moceller, T.; Baila, J. C., Jr.; Kleinberg, J.; Guss, C. O.; Castellion, M. E.; Metz, C. *Chemistry with Inorganic Qualitative Analysis*; Academic Press: New York, 1980; p 1061.
(16) Moceller, T.; Bailar, J. C., Jr.; Kleinberg, J.; Guss, C. O.; Castellion, M. E.; Metz, C. *Chemistry with Inorganic Qualitative Analysis*; Academic Press: New York, 1980; p 1066.

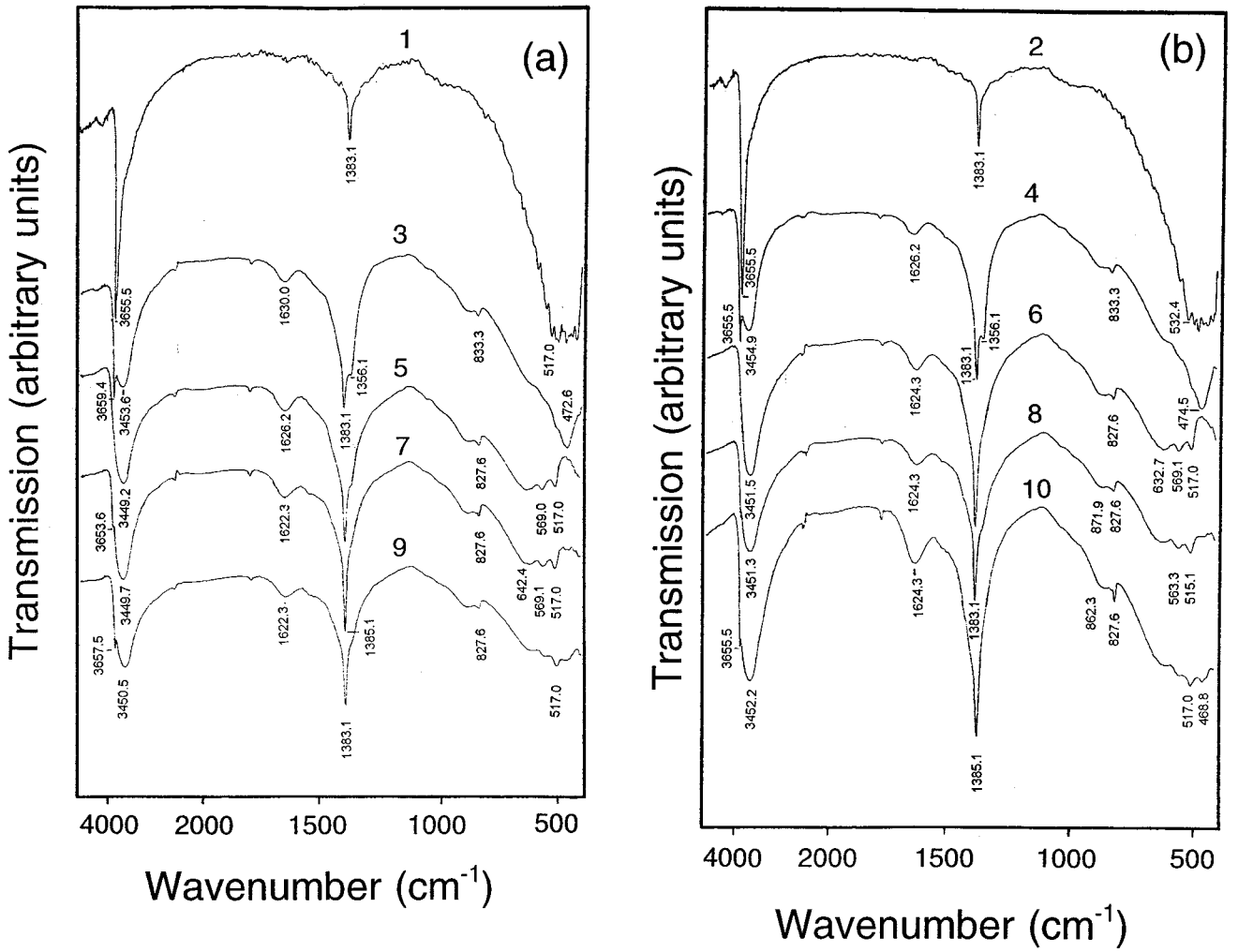

Figure 3. FTIR spectra for two series of samples: (a) samples 1, 3, 5, 7, and 9, dried at 25 °C for 18 h, and (b) samples 2, 4, 6, 8, and 10, dried at 60 °C for 18 h.

product (K_{sp}) analysis for $Co(OH)_2$, $Co(OH)_3$, and $Mg(OH)_2$ cannot give a good account for the observed Co/Mg ratio variation. Finally, it should be mentioned that after hydrothermal treatment for 18 h (Table 1), the reaction system is in equilibrium under the set experimental conditions.

Formation of Hydrotalcite-Like Phase. In the ammoniacal solution, Mg^{2+} and Co^{2+} are coprecipitated into the solid phase. This is evidenced in the FTIR spectra of Figure 3 for room-temperature-dried samples. For instance, in the sample using nitrogen as the background atmosphere, a sharp and strong peak located at 3655.5 cm^{-1} is assigned to hydroxyl group ν_{O-H} vibration of the metal hydroxide.[4,17,18] Since it sits between that of brucite (3698.0 cm^{-1}) and $Co(OH)_{2,3}$ (3632.4 cm^{-1}),[10] a mixing between Mg^{2+} and Co^{2+} in the brucite-like hydroxide (sample 1) is confirmed. The 1383.1 cm^{-1} peak in the same sample is assigned to the vibration mode (ν_3) of the NO_3^- anion.[19,20] The band at lower wavenumber around 474 cm^{-1} is attributed to metal−oxygen vibration absorptions.[1,21]

It is noted that the found ν_3 mode of NO_3^- (1383.1 cm^{-1}) departs slightly from that at 1340−1380 cm^{-1} for unperturbed nitrate ions.[20] Interestingly, with an increase of O_2 partial pressure, intensities of the ν_3 mode of NO_3^- in the samples 3, 5, 7, and 9 are sharply increased, indicating a significant increase of the anions in the precipitates. In sample 7, this peak is shifted to 1385.1 cm^{-1}, which is further away from the unperturbed case. Starting from the sample 3 onward, a second NO_3^- peak (ν_2 mode) can be seen at 833.3 cm^{-1}.[1,20,22] In addition to the NO_3^- anions, CO_3^{2-} anions are also detected. A shoulder peak, ν_3 mode of CO_3^{2-},[1,19,20,22] is observed clearly at 1356.1 cm^{-1} for the spectrum of sample 3. This peak, together with a ν_2 band at around 862.3−871.9 cm^{-1} in the samples 3−10, confirms the presence of CO_3^{2-} that results from atmospheric CO_2 dissolution. Since no ν_1 vibration absorption (around 1050 cm^{-1} for both anions[1,19,20,22]) is found, it can be concluded that both anions have a planar symmetry of D_{3h}, though they have been slightly perturbed by their adjacent chemical entities such as interlayer water.

Regarding the structural location of the above two anions, the presence of simple metal salts or contami-

(17) Grey, I. E.; Ragozzini, R. *J. Solid State Chem.* **1991**, *94*, 244.
(18) Ulibarri, M. A.; Hernandez, M. J.; Cornejo, J. *J. Mater. Sci.* **1991**, *26*, 1512.
(19) Chisem, I. C.; Jones, W. *J. Mater. Chem.* **1994**, 4, 1737.
(20) Kruissink, E.; van Reijen, L. L.; Ross, J. R. H. *J. Chem. Soc., Faraday Trans.* 1 **1981**, *77*, 649.
(21) Busca, G.; Trifiro, F.; Vaccari, A. *Langmuir* **1990**, *6*, 1440.
(22) Fernandez, J. M.; Barriga, C.; Ulibarri, M. A.; Labajos, F. M.; Rives, V. *J. Mater. Chem.* **1994**, *4*, 1117.

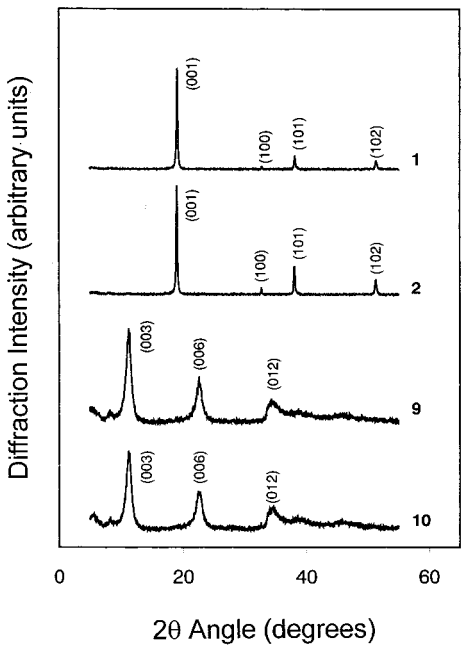

Figure 4. XRD patterns for the nitrogen-synthesized samples (1 and 2) and the oxygen-synthesized samples (9 and 10).

nants (such as carbonate) cannot be totally ruled out, although all samples had been thoroughly washed. As observed in the elemental analysis, the amount of these anions increases with the partial pressure of O_2. It is naturally thought that the increase in anion population is due to more and more original Co^{2+} being converted to Co^{3+} with the increase of P_{O_2}. Furthermore, it is recognized that the observed wavenumbers for the two types of anions are similar to those reported for HTlcs.[1,19,20,22] Hence, both EA and FTIR findings all suggest a formation of HTlcs in these precipitates, which will be confirmed next by a structural method, XRD.

As evidenced in Figure 4, the samples (1 and 2, Table 2) prepared in a nitrogen atmosphere have a brucite-like structure,[10] while samples 9 and 10 prepared in pure oxygen, have a typical XRD pattern of HTlcs.[1,19,22] This brucite-like phase to HT-like phase transformation clearly occurs with the increase of the oxygen content in the preparative atmosphere. For low oxygen partial pressure synthesis (samples 3 and 4), both brucite-like and HT-like phases are detected by XRD, which is in good agreement with the FTIR result that the brucite-like OH absorption (3659.4 cm^{-1}) is still observable in such cases. From the sample 5 onward, with the increase of P_{O_2} in the synthesis (samples 5−10), the only crystallographic structure recognizable is the HT-like. Since the HTlc formation is confirmed, the intercalated anions (NO_3^-) in the interlayer spacing now can be assigned to lie parallel to the brucite-like sheets in view of the planar D_{3h} symmetry found in the FTIR study. In connection with hydrogen bonding, the content of water molecules in these HTlcs also increases with the intercalated anions (see Table 2; about one water molecule per compound). The O−H stretching absorptions at 3453.6−3449.2 cm^{-1} and bending vibration mode δ_{H-O-H} over the 1630.0−1622.3 cm^{-1} can be clearly identified.[4,19,22] It should be mentioned that the brucite-like OH vibration is barely visible in samples 3, 5, 7, and 9. This indicates that both a structural conversion (from brucite-like type to HTlc) and a water intercalation occur upon introduction of oxygen to the sample preparation (Table 2). Although sample 1 (and similarly sample 2) was prepared in nitrogen, the presence of NO_3^- is found in its FTIR spectrum (Figure 3). This observation can be attributed to an encapsulation of NO_3^- during the precipitation or to a trace of HTlc in the two samples. The latter assignment would suggest a small degree of Co^{2+} oxidation during the synthesis, since the water used was not totally deoxygenated.

For the samples dried at a higher temperature (samples 2, 4, 6, 8, and 10), FTIR spectra (Figure 3) reveal similar findings as their counterparts (samples 1, 3, 5, 7, and 9). However, the weakening of the XRD peak intensity (Figure 4) is observed, which suggests a structural degradation of HTlcs after the prolonged drying at 60 °C (e.g., sample 10). Although the XRD investigation gives no evidence of Mg−Co spinel oxide formation, the weak IR absorptions at 632.7 and 569.1 cm^{-1} in sample 6 (and similarly in the samples 5−9 and 8−10 over the same wavenumber region) are attributable to the presence of Mg-modified Co_3O_4 (pure Co_3O_4 phase observed at 661 and 568 cm^{-1} [23,24]). Similar conclusion had been proposed in the Co−Al-HTlcs, which suggested that there is a phase of well-dispersed Co_3O_4 that shows no XRD lines (i.e., nondetectable by the XRD technique).[3] Judging from the low intensities of the two IR peaks, one can realize that the Co_3O_4 phase should be very small if present. It is noted when the coprecipitates are hydrothermally treated at higher temperatures, the observed HTlc phase is gradually converted to a Co_3O_4 type spinel phase at 90−100 °C.

The extra charge that a Co^{2+} gains during the oxidation to Co^{3+} is +1. In HTlcs, these extra positive charges will be balanced by the negative charges of interlayer anions to keep total electric neutrality for the solid. It is found that anion population (NO_3^-) increases with the O_2 partial pressures used in the preparation. Interestingly, this anion increase has a very similar trend as that shown in Figure 2 for $-\Delta G$ versus P_{O_2} data (from eq 4). Nevertheless, although the thermodynamic property ΔG can be associated with the chemical equilibrium constant, the exact expression is not intended to be obtained here due to the complexity of the current case.

The chemical formula determined for the samples 9 and 10 is $Mg_{0.3}Co^{II}_{0.6}Co^{III}_{0.2}(OH)_2(NO_3)_{0.2}\cdot H_2O$ (Table 2). In these two samples, the Co^{3+}/NO_3^- ratio is about 1, which meets well the charge neutrality for the HTlcs. The trivalent cation to total cation ratio $Co^{III}/[Mg^{II} + Co^{II} + Co^{III}]$ is 0.2 for these two compounds, which is in the lower end of required range 0.2−0.4 for HTlc formation.[1] Nevertheless, it should be mentioned that the above formula assumes no Co_3O_4 and $Co(OH)_3$ [or CoO(OH)] formation. In fact, as mentioned earlier, the FTIR study has suggested that there might be a trace amount of Co_3O_4 formed in samples 3−10.

Thermal Decomposition and Surface Areas. Although different drying temperatures only cause subtle modifications in FTIR spectra and XRD patterns, the temperature variation in drying alters the thermal

(23) Lutz, H. D.; Feher, M. *Spectrochim. Acta A* **1971**, *27*, 357.
(24) Preudhomme, J.; Tarte, P. *Spectrochim. Acta A* **1971**, *27*, 1817.

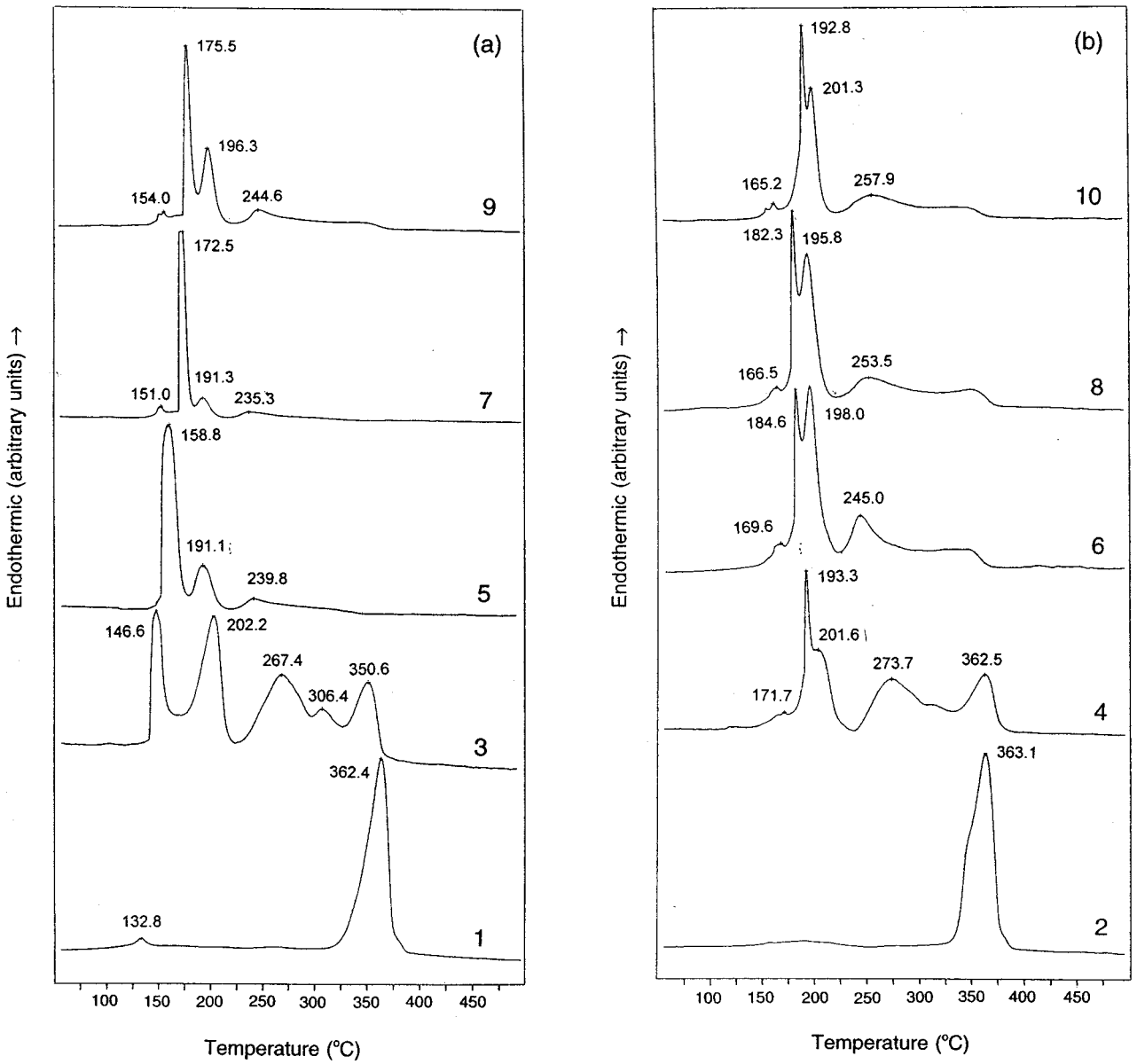

Figure 5. DSC curves for two series of samples: (a) samples 1, 3, 5, 7, and 9, dried at 25 °C for 18 h, and (b) samples 2, 4, 6, 8, and 10, dried at 60 °C for 18 h.

behavior of samples significantly. In Figure 5, DSC curves for the room-temperature-dried and 60 °C-dried samples are plotted, respectively. For sample 1, a small endothermic peak at 132.8 °C can be assigned to dehydration of sample surface water or of interlayer water,[1,25] as discussed earlier. In line with FTIR/XRD results, the removal of hydroxy groups (collapse of overall brucite-type structure) occurs at a high-temperature endothermic peak around 362.4 °C, which is rather brucite-like.[10] From sample 3 onward, the interlayer water increases significantly, reflecting the formation of HTlcs. In the DSC curve for sample 3, the endothermic peak at 146.6 °C is due to the dehydration of interlayer water. The second endothermic at 202.2 °C is assigned to decomposition of the HTlc phase, i.e., removal of hydroxyl groups. In view of the presence of brucite-type structure in this sample (FTIR/XRD results), the peak at 350.6 °C is attributable to decomposition of the brucite-type phase, noting that this peak is located near the similar peak (362.4 °C) in sample 1. Other two peaks at 267.4 and 306.4 °C can be assigned to decompositions of NO_3^- and CO_3^{2-}, respectively, as they are common temperatures for anion decomposition.[19,25]

With an increase of partial pressure of O_2 in synthesis, the distance between the first and second endothermic peaks narrows. As shown in the sample 5, the dehydration peak is now located at 158.8 °C, while the decomposition of HTlc shifts to 191.1 °C. The endothermic band/tail at 239.8 °C as well as those of samples 7 and 9 are assigned to decomposition of NO_3^- and CO_3^{2-},[19,25] similar to the assignments for sample 3. Since no brucite-type structure is detected, high-temperature peaks, such as 362.4 °C in sample 1 and 350.6 °C in sample 3, are not observable in samples 5, 7, and 9. Starting from sample 7, the dehydration peaks separate into two components. The first one (151.0 °C in sample 7 and 154.0 °C in sample 9) is considered

(25) Pesic, L.; Salipurovic, S.; Markovic, V.; Vucelic, D.; Kagunya, W.; Jones, W. *J. Mater. Chem.* **1992**, *2*, 1069.

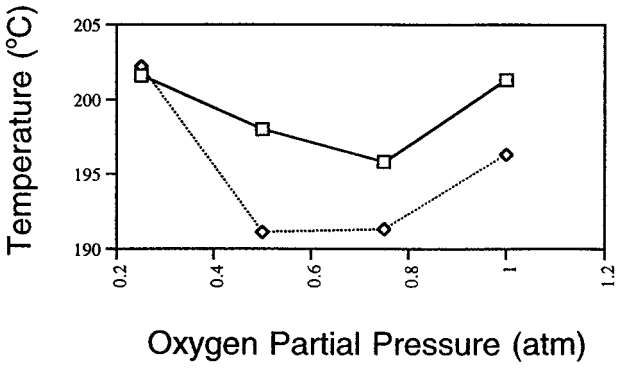

Figure 6. Decomposition temperature versus O_2 partial pressure (Table 1) for samples 3, 5, 7, and 9 (◇) and samples 4, 6, 8, and 10 (□) note that the Co/Mg molar ratios in samples 3, 4, 9, and 10 are lower than those in samples 5, 6, 7, and 8.

somehow like that in samples 3 and 5. The second component (172.5 °C in sample 7 and 175.5 °C in sample 9), however, reveals that water molecules have been bounded more strongly in these HTlcs. Presumably, they are bound to some defect sites in the layered structure that may thus result in a higher bonding energy.

When they were dried at 60 °C, the overall DSC curves of samples 2, 4, 6, 8, and 10 seem to be considerably "drier", which has been evidenced in the EA data of Table 2. For instance, the first endothermic peak is not observable in sample 2, whereas it is at 132.8 °C in sample 1 (25 °C dried). The low-temperature dehydration peaks in samples 4, 6, 8, and 10 shift to the higher temperature region (165.2−171.7 °C) compared to those (146.6−158.8 °C) in samples 3, 5, 7, and 9. Upon the 60 °C-drying, the singlet peaks at 146.6 and 158.8 °C observed in samples 3 and 5, respectively, are now separated into two components in samples 4 and 6. On the basis of this observation, the speculation of defect site bonding for water is further validated, since prolonged drying of the samples at 60 °C results in poorer XRD pattern; i.e., a less ordered structure is generated.

For the 60 °C-dried sample 2 (nitrogen-prepared), the brucite-type structure has gone at 363.1 °C, which is very similar to that of the 25 °C-dried sample. As for the thermal stability of the oxygen-prepared samples, it is found that HTlcs with lower Co/Mg ratios are more stable regardless of the postsynthesis drying treatment. As mentioned earlier, the Co/Mg ratios in samples 1−4, 9, and 10 are lower than those in samples 5, 6, 7, and 8. This is reflected in the decomposition temperature (i.e., removal of hydroxy groups) profiles in Figure 6 for the two series of samples. A simple explanation of this is that with sufficient Mg^{2+} cations in the brucite-type sheets, a better layered structure can be built, noting that the brucite structure [$Mg(OH)_2$] is thermally more stable.[1,10]

Concerning chemical applications of these HTlcs, it would be useful to study specific surface areas of samples upon thermal treatments. As shown in Figure 7, in low-temperature decomposed samples (at 200 °C for 45 min), data of specific surface areas are scattered

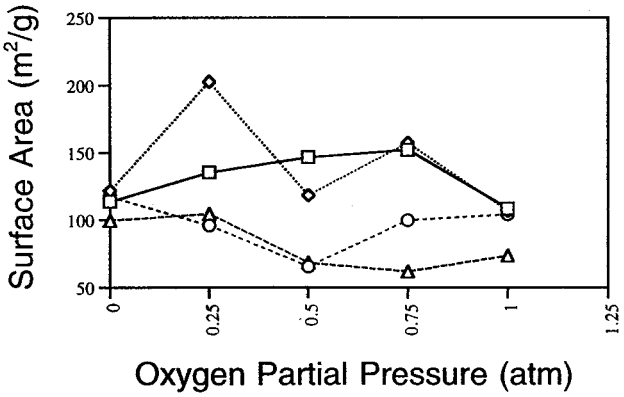

Figure 7. BET measurements for the calcined samples: (i) samples 1, 3, 5, 7, and 9 (□) at 200 °C for 45 min, (ii) samples 2, 4, 6, 8, and 10 (◇) at 200 °C for 45 min, (iii) samples 1, 3, 5, 7, and 9 (○) at 400 °C for 60 min, and (iv) samples 2, 4, 6, 8, and 10 (△) at 400 °C for 60 min.

for the 60 °C-dried samples (2, 4, 6, 8, and 10, which are somehow degraded), because these precipitate have not been converted to stable Co−Mg oxides at 200 °C. Nevertheless, when the HTlcs are calcined at 400 °C for 60 min, formations of stable Co−Mg oxides are expected on the basis of the observed DSC data. The general trend here is that the specific surface areas are lower for the samples with low Mg content (such as samples 5 and 6, which have high Co/Mg ratios). This observation is consistent with the thermal decomposition behaviors of the samples revealed in the DSC study.

Conclusions

In summary, non-Al-containing brucite-like compound and HTlcs of $Mg_aCo^{II}_bCo^{III}_c(OH)_d(NO_3)_e(CO_3)_f\cdot nH_2O$ have been synthesized for the first-time by coprecipitation and hydrothermal treatments with controlled O_2:N_2 atmospheres. The synthesized compounds have been characterized with EA, FTIR, XRD, DSC, and BET techniques. On the basis of EA/XRD investigations, it has been found that 23% of Co^{2+} is oxidized to Co^{3+}. Anion species, such as NO_3^-, are intercalated in brucite-type layers of HTlcs. The anion intercalation increases with the rise in O_2 partial pressure. In response to an increase of O_2 partial pressure, the XRD pattern shows a brucite-like to hydrotalcite-like structure conversion. By varying drying temperature (25 °C and 60 °C) and using a DSC method, it has been revealed that the thermal stability of HTlcs increases with Mg content. Higher specific surface areas are observed for the decomposed HTlcs with higher Mg content. Trace Co_3O_4 is also detected in FTIR analysis for samples synthesized under high O_2 partial pressures, resulting from a deeper oxidation of Co^{2+} in the HTlc precipitates.

Acknowledgment. The authors gratefully acknowledge research funding (RP960716) supported by the Ministry of Education and National Science and Technology Board of Singapore and the technical assistance provided by Ms. S.C. Yu.

CM9802503